PNAS
www.pnas.org

Supplementary Information for

Histone Methyltransferase Smyd1 Regulates Mitochondrial Energetics in the Heart

Junco Shibayama Warren
Email: junco.warren@utah.edu

This PDF file includes:

Supplementary text
Figs. S1 to S9
Captions for databases S1 to S11
References for SI reference citations

Other supplementary materials for this manuscript include the following:

Datasets S1 to S11

www.pnas.org/cgi/doi/10.1073/pnas.1800680115

Supplementary Information Text

Methods

Ethics Approval

The experimental protocol conformed to the Guide for the Care and Use of Laboratory Animals (The National Academy Press, 8th edition, 2010) and was approved by University of Utah IACUC. All efforts were made to minimize pain and distress during isolation of the heart by deep anesthesia. In this study, we used both male and female transgenic mice on a C57BL/6 background and minimized the number of animals used.

Animals and Sample Collection

Inducible, cardiac-specific Smyd1-KO mice ($Smyd1^{flox/flox}$ $Cre^{+/-}$) were developed as described previously (1). These animals ($Smyd1^{flox/flox}$ $Cre^{+/-}$), as well as control mice, which lacked the Cre allele ($Smyd1^{flox/flox}$ $Cre^{-/-}$) ages 8-10 weeks were fed a diet containing tamoxifen, 0.4 mg/g of chow diet (Harlan, Cat#: TD.07262) for 5 weeks to achieve deletion of the Smyd1 gene. After 5 weeks of tamoxifen chow the mice were returned to a normal diet and monitored via echocardiography for 14 weeks. For this study, tissue from the ventricles was harvested after 3 weeks and 5 weeks of tamoxifen diet, which was immediately frozen in liquid nitrogen and stored at -80°C until they were used for metabolomic and proteomic analyses and gene expression studies.

Metabolomic Analyses

Ventricular tissue samples harvested at week 3 from Smyd1-KO mice and control animals were analyzed using gas chromatography-mass spectrometry (GC/MS) and direct infusion tandem mass spectrometry (MS/MS) at the University of Utah Metabolomics Core Facility and ARUP Laboratories (Salt Lake City, UT), as described previously (2). Quantitative measurements of TCA cycle intermediates, lactic, pyruvic, and 3-OH butyric acids were performed at ARUP Laboratories. Briefly, dried extract from 50 mg of cardiac tissue was deproteinized with acidified methanol. Organic acids were oximated and converted to volatile trimethylsilyl (TMS) derivatives before analysis by GC/MS (3). Compound identification was obtained by retention time and characteristic fragmentation spectra using Agilent MassHunter software. Organic acids were quantified using a six-point calibration curve with 2-ketocaproic acid as internal standard. Ventricular samples from week 5 were analyzed using two metabolomic platforms (GC/MS and HILIC-QTOF/MS) for metabolomic screening, which were performed in the NIH West Coast Metabolomics Center at the University of California, Davis, as described previously (4, 5).

Bioinformatics: Analysis of the metabolomic and lipidomic data was carried out using Metaboanalyst 3.0 software (6-8) including the generation of heat maps and Pathway Impact Analysis (**Figure 2C**), which maps metabolic pathways and their associated p-values (from pathway enrichment analysis), where node color is based on the p-value and node radius is determined from the pathway impact value. Differences in the abundance of individual metabolites were determined using a Student's t-Test (2 tails, unpaired comparison). A value of $p<0.05$ was considered statistically significant. Data are given as mean ± SEM.

Proteomic Analysis

Proteomic analysis of ventricular tissue collected from Smyd1-KO and control mice, at week 3 and week 5, was conducted using label-free quantitative LC-MS/MS, as described in our previous publication with some modification (2). Briefly, the extracted proteins from frozen ventricular tissue samples were reduced, alkylated, then digested with trypsin (1 μg trypsin: 40 μg proteins) overnight at 37°C on the filter in a humid environment. Peptides were analyzed on an Orbitrap Velos Pro mass spectrometer interfaced with an EASY-nlc nLC1000 UPLC outfitted with a PicoFrit reversed phase column (15 cm x 75 um inner diameter, 3 μm particle size, 120 Å pore diameter, New Objective). Data were searched against the mouse Uniprot database using the database search algorithms in the PEAKS 7.5 Studio software. False discovery rate was 1.0%. Searches allowed for ≤3 missed cleavages, with Carbamidomethylation set as a fixed modification and oxidation (M), methylation (KR), dimethylation (KR), and trimethylation (K) as variable modifications.

Label-free quantitation of protein expression was accomplished using the PEAKS 7.5 Studio software. For PEAKS analyses, peptide features across the entire chromatographic run for each sample were aligned between MS runs and between control and KO samples with a mass error tolerance of 15 ppm and a retention time shift tolerance of 5 minutes. Protein normalization factors were calculated in PEAKS from the total ion current of each sample and applied to the protein areas determined by the PEAKS label-free quantification algorithms. Fold change (FC) for each protein was determined from a ratio of the average protein area of KO samples to the average protein area of control samples and the significance of this change was determined by a Student's t-Test of control and KO areas. Proteins identified by at least 1 unique peptide and 2 or more total peptides, with a p-value less than 0.01, were considered significant. Unbiased enrichment analyses in biological process, cellular component, and KEGG pathway were performed using the STRING database (9). The terms were sorted by their enrichment p-value, which were computed using a Hypergeometric test (10) and corrected for multiple testing using the method of Benjamini and Hochberg (11).

Mitochondrial Respirometry Analysis

Ventricular mitochondria were isolated from Smyd1-KO and control mice by differential centrifugation as described previously with minor modifications (12). The final pellet of the mitochondrial fraction was re-suspended in the Mito Isolation Solution (MSHE) with 0.5 % BSA. After estimating the concentration by BCA protein assay (without BSA), 10 μg of mitochondria in the Mitochondrial Assay Solution (MAS)-1 with 0.5 % BSA were placed in each well of the Seahourse XF24 plates (Agilent Technology) with pyruvate (5 mM) and malate (5 mM) or palmitoyl-carnitine (40 μM) and malate (5 mM) as a substrate to test glucose/pyruvate and fatty acid oxidation, respectively. Mitochondrial respiration was calculated as the O_2 consumption rate (OCR), sensitive to 2.5 mM exogenous ADP, 2 μM rotenone, 4 μM antimycin A, and 4 μM Carbonyl cyanide-4-(trifluoromethoxy)phenylhydrazone (FCCP).

Cell Mito Stress Test

An extracellular flux analyzer (Seahorse XF^e96, Agilent Technologies) was used to assess mitochondrial function as described previously (13) with some modifications.

H9c2 cardiomyocytes were plated in 96-well Seahorse analyzer plates (2 x 10^4 cells/well). After incubation for ~18 hours, the cells were transduced with adenovirus and/or transfected with siRNA. After 48 hours, the measurements of oxygen consumption rates (OCR) were conducted in XF base medium (Agilent-Seahorse) pH 7.4 supplemented with 2 mM L-glutamine, 1 mM pyruvate and 25 mM glucose. OCR was measured prior to and after the sequential addition of oligomycin (1uM), carbonyl cyanide 4-(trifluoromethoxy) phenylhydrazone (FCCP, 5 μM) and rotenone (1 μM) and antimycin A (1 μM). Following the completion of OCR measurements, cells were stained with Hoechst 33342 to stain nucleus (Thermo Fisher Scientific, Cat#H3570, 1:500 dilution in PBS). The intensity of nuclear staining per well was determined using BioTek Cytation 5 (excitation at 360 nm, emission at 450 nm, (14)), and OCR values were normalized to the intensity of nuclear staining. Three readings were taken after each injection of the following compounds, and following parameters were calculated as average of the three time-points: (1) The Basal OCR (measurement obtained before the addition drugs). (2) OCR coupled to ATP production (the difference between the basal OCR and the OCR recorded after the addition of oligomycin). (3) the spare respiratory capacity (the difference between basal OCR and FCCP-induced OCR). In the palmitate oxidation assays, cells were incubated with GlutaMAX substituted with 0.5 mM carnitine and 1% FBS for 24 hours prior to assays, followed by incubation with either palmitate (160 μM) coupled to BSA or BSA alone in Krebs-Hanseleit buffer pH 7.4 containing 0.5 mM L-carnitine and 5 mM HEPES. The OCR in response to oligomycin, FCCP and Rotenone plus Antimycin A was measured as describe above. Statistical analysis was performed using One-way ANOVA with Newman-Keuls post-hoc test for pairwise comparisons (Addinsoft Inc., www.xlstat.com). The shuttle and mammalian expression vector for Flag-tagged PGC-1α (pDC316-Flag-PGC-1α) that was used in mitochondrial stress test were generated by insertion of Flag tagged mouse PGC-1α cDNA into pDC316 (Microbix). Adenovirus harboring Flag-PGC-1α was made using AdMax system (Microbix) with pDC316-Flag-PGC-1α. Overexpression of PGC-1α was confirmed by RT-PCR (Figure S6A).

Isolated Neonatal Rat Cardiomyocytes

Neonatal rat ventricular myocytes (NRVMs) were isolated from Sprague-Dawley neonatal rats (0-1 day old) as described previously (15). Briefly, NRVMs were obtained by enzymatic dissociation from 0-1 day old litters and plated in DMEM media (Invitrogen, #11965) containing 1% penicillin, 1% streptomycin, 1% insulin-transferrin-sodium selenite supplement and 10% fetal bovine serum for the first 24 hours after which the cells were cultured in serum-free media. For the loss-of-function study of Smyd1, NRVMs were transfected with Smyd1-siRNA (Qiagen, Cat#SI02021775) and scrambled-siRNA (Qiagen, Cat#1022076) using lipofectamine RNAiMAX reagent (Invitrogen, Cat#13778) based on the manufacturer's instructions. 20 μM siRNA was transfected unto $1.5x10^6$ cells in 6 cm dishes. siRNA and lipofectamine were individually incubated in conical tubes containing OPTI-MEM media (GBCO) at room temperature for 5 min, mixed and incubated at room temperature for 20min. siRNA/lipofectamine mixtures (500 μl/dish) were added to culture dishes. Cells were cultured either for 24 or 48 hours and were harvested for RT-PCR, western blotting, and proteomic analyses. For the overexpression study, NRVMs were treated with adenovirus expressing either Flag-

tagged mouse Smyd1(a), Smyd1(b) or an empty virus (control) at a multiplicity of infection (MOI) of 25.

Gene Expression Analysis

Real-time PCR was performed using Taqman primers as described previously (16). Briefly, RNA was extracted using TRizol (Life Technologies), followed by ethanol extraction. Reverse transcription was performed from 1ug of RNA using QuantiTect Reverse Transcription Kit according to the manufacture's instruction (Qiagen). Taqman primers are as follows: *Smyd1*: Mm00477663_m1 and Rn00477666_m1; *Ppargc1a*:Mm01208835_m1 and Rn00580241_m1; *Ppargc1b*:Mm00504730_m1 and Rn00598552_m1; *Ppara*:Mm00440939_m1 and Rn00566193_m1; *Rxra*:Mm00441185_m1 and Rn00441185_m1: NRF1:Mm01135606_m1 ; Sirt1:Mm01168521_m1 ;*Cd36*:Mm00432403_m1; *Pdk4*:Mm01166879_m1; *Acox1*:Mm01246834_m1; *Acadm*:Mm01323360_g1; *Dld*: Mm00432831_m1; *Pdhb*:Mm00499323_m1; *Ppm1k*:Mm00615792_m1; *Slc22a5*:Mm00441468_m1; *Ppm1k*:Mm00615792_m1. The Cq values from the targeted genes were normalized by the gene expression level of *Tbp (*Mm00446971m1, Rn01455646_m1).

Western Blot Analysis

Western blot analysis was carried out as previously described (1). The expression of Smyd1, PGC-1α, PGC-1β, PPARα, and RXRα was detected using rabbit anti-Smyd1 antibodies (Abcam, Cat#: ab32482; ab54481; ab176328; ab24509; ab125001) with 1:5000 dilution for Smyd1 and 1:1000 for PGC-1β, PPARα, and RXRα, followed by goat anti-rabbit secondary antibody (Jackson ImmunoResearch Laboratories, Inc. #711-035-152) with 1:5000 dilution. The signal was normalized to either actin (Santa Cruz, #sc-1616) or β-tubulin (Abcam, # ab6046).

ChIP-PCR. ChIP was performed using the commercially available ChIP-IT kit (Active Motif, 53040) according to manufacturer's instructions. Briefly, ventricular tissue from control and Smyd1-KO mice was minced into small pieces and fixed by incubating with a fixation solution containing 1% formaldehyde at room temperature for 15 min. After centrifugation at 1,500 g for 1 min and washing the pellets with cold PBS, tissue was lysed in a Chromatin Prep Buffer, followed by sonication to fragment DNA between 300 and 1,000 bp. DNA-bound proteins were immunoprecipitated using anti-H3K4me3 (Abcam, ab8580) and anti-H3K9me1 (Abcam, ab9045). ChIP was performed using Protein G agarose beads, ChIP filtration columns, and ChIP buffer provided in the ChIP-IT kit. The DNA recovered was analyzed by RT-PCR using primer sets (see a table below) that amplified the promoter regions of PGC-1α, PGC-1ß, PPARα, and RXRα. PCR was performed in duplicate with equal amounts of specific antibody-immunoprecipitated samples and Input. Values were normalized to input measurements, and enrichment was calculated using the ΔΔCt method.

Pppargc1a (PGC-1α)

Primer 1 (-1kb)	Left	GCCTGGAAGGGTTAAGTCTG
	Right	CAATGAGGGGTAATGCAGGT
Primer 2 (-0.1kb)	Left	GACGTCAGGAGTTTGTGCAG
	Right	GACGCCAGTCAAGCTTTTTC
Primer 3 (1kb)	Left	ACACAAGCAGTTTCCCCGTA
	Right	GGGTCCATCTCACCAGAGTC
Primer 4 (2kb)	Left	TCAGCGTCCAGCCTTAGATT
	Right	ATGGAAGCTGCCCACACTAC
Primer 5 (3kb)	Left	TCTCCCCTCATCTCTGTGCT
	Right	GTAACAATCCCAAGGCTCCA

Ppargc1b (PGC-1β)

Primer 1 (-3kb)	Left	CCCTCTGGATAATGCAGTCA
	Right	CCCACCAAGGATCTGAATGT
Primer 2 (0.5kb)	Left	GTTACAGGCGTAGCGAGCTG
	Right	AGGACGCGCCTACAACAC
Primer 3 (1.5kb)	Left	GGCCATAGCTCTCTGCAAAC
	Right	CTTGGGCCTCTGCTATGAAC
Primer 4 (5kb)	Left	TACTCTTGCCGTTCATGTGC
	Right	CGGATCCCAGTCATTTCTGT

PPARα

Primer 1 (-1kb)	Left	AACCAAGCACCCTCTCTTCA
	Right	CCTTGCACAGTGACCTGTCT
Primer 2 (-0.5kb)	Left	TGCGATCTAGACCAGCTCAA
	Right	GAAGGGACTGCCCAAGGT
Primer 3 (1kb)	Left	TGGAGACCCACAGCCACT
	Right	CTCCAGTTCCAGGACTCCAC
Primer 4 (2.5kb)	Left	TGGGTTTGAGTCAACAGCAG
	Right	AGCCACTGCACAGAGGAGAC

RXRα

Primer 1 (-1.3kb)	Left	CTGCCCATCTTAACCACACC
	Right	GGATCAGGAAAGGTCTGTGG
Primer 2 (-0kb)	Left	TGTTAGGTGAAGGGGACTGG
	Right	CGCGGACACACAAAGAGG
Primer 3 (1.3kb)	Left	GCTCTAGCTATCCGGGAACC
	Right	GCCTTCTCCAAGCCACAG
Primer 4 (5kb)	Left	CAGGGAAATTGCACCCTAGA
	Right	CCTCATGGTAGCGTGGAAAG

Luciferase Reporter Assay. H9c2 cells were grown in DMEM (Corning Cellgro) supplemented with 10% FBS and 1% penicillin/ streptomycin on white 96-well plates. The cells were also incubated in clear 96-well plates to ensure the cell confluency and quality after transfection. At 70% confluence, the cells were infected with either Ad-CMV-Null (empty virus) or Ad- Smyd1A-Flag adenovirus at a multiplicity of infection (MOI) of 300. After 48 h, the cells were transfected with 50 ng/well of human Ppargc1A (SwitchGear Genomics, Prod#S722424), Ppargc1B (SwitchGear, Prod#S705203), negative control (scrambled, SwitchGear Genomics, Prod#S790001), or positive control (ACTB, SwitchGear, Prod#S717678) luciferase reporter construct (SwitchGear Genomics) using with 8 ng/well of a pGL4 13 [luc2 SV40] vector (Promega Corporation, Cat#E668A) and incubated for 24 h. Luciferase activity was assayed using the Light-Switch Luciferase assay reagent (SwitchGear Genomics, Cat#E1910) according to the manufacturer's instructions and measured using a Veritas microplate luminometer (Thuner Biosystems, Inc).

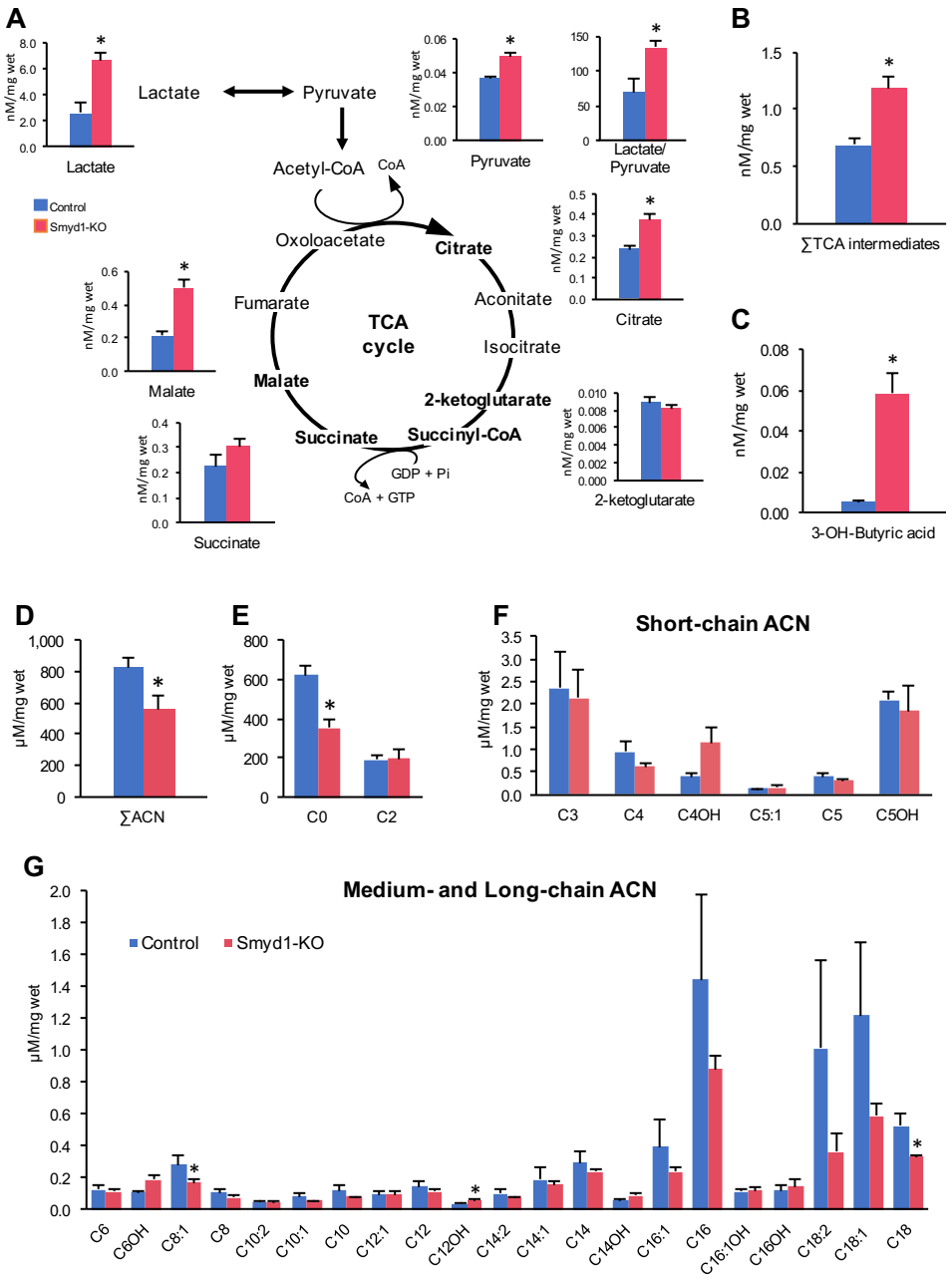

Fig. S1. Targeted quantitative analysis of organic acids involved in the lactate/pyruvate oxidation pathways and the TCA cycle and acylcarnitine species. A, Metabolite profiles showing lactate, pyruvate, and organic acid intermediates within the TCA cycle. **B,** Total pool of TCA-cycle intermediates. **C,** 3-hydroxybutyric acid, an intermediate of ketone body metabolism. **D-G,** Levels of the total pool of acylcarnitine species (ΣACN, Panel D), free carnitine (C0, Panel D), and short-chain (Panel F), and medium- and long-chain acylcarnitine species (Panel G) isolated from the Smyd1-KO and control hearts. Acyl chain lengths are denoted by the numbers. Acylcarnitine species that represent monohydroxylated (OH) are also shown. (n=4 in control, n=6 in Smyd1-KO), *: $p<0.05$

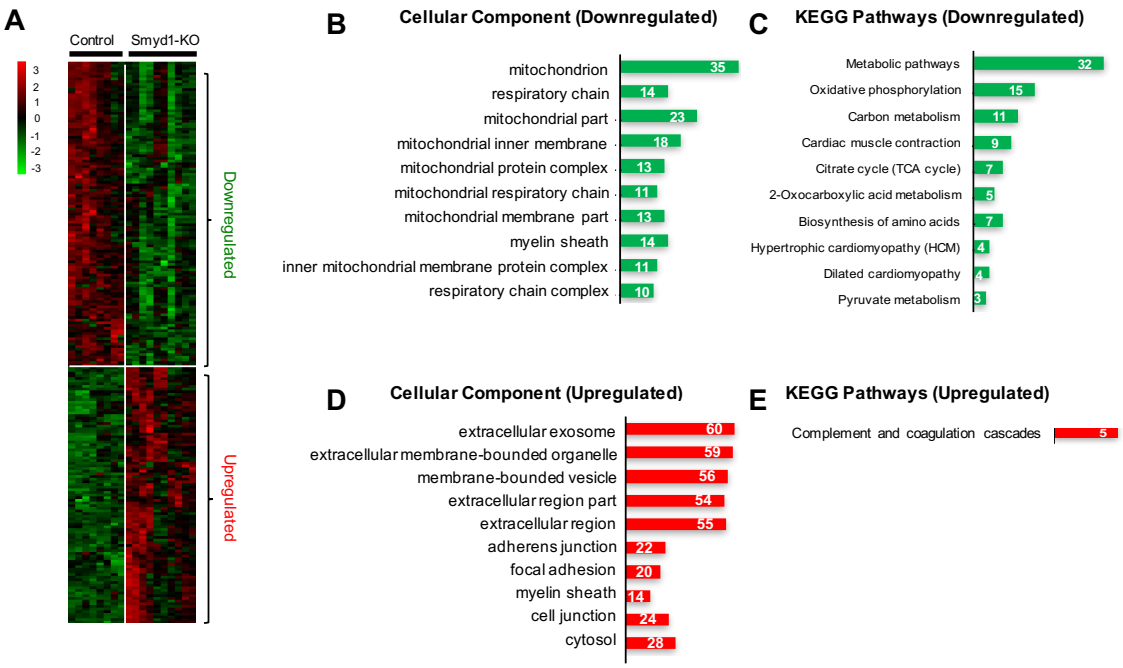

Fig. S2. Upregulated and downregulated proteome of the Smyd1-KO heart (week 3) compared with the control heart. **A,** The heat map represents all proteins that were differentially expressed in Smyd1-KO mice (115 downregulated proteins, 97 upregulated proteins, $p<0.01$). **B-C,** Enrichment analyses of significantly downregulated proteins for GO term cellular components **(B)** and KEGG pathways **(C)**. **D-E,** Enrichment analyses of significantly upregulated proteins for GO term cellular components **(D)** and KEGG pathways **(E)**.

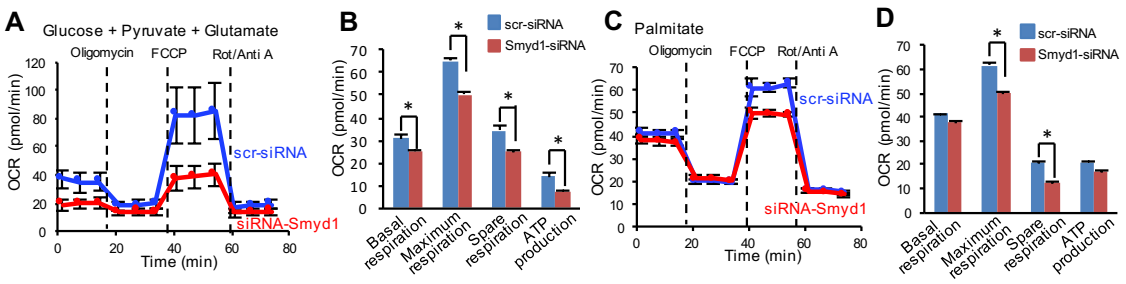

Fig. S3. Reduced mitochondrial respiration capacity induced by silencing Smyd1 gene in H9c2 cardiomyocytes. A-B, H9c2 cells were transfected with Smyd1-siRNA for 48 hours, and the oxygen consumption rates (OCR) were measured in XF base medium pH 7.4 supplemented with 25 mM glucose, 1 mM pyruvate, and 2 mM L-glutamate. Respiration parameters were determined as described in the methods in Supporting Information. **C-D,** Palmitate oxidation was measured in Smyd1 knockdown cells by incubating with palmitate (160 µM) coupled to BSA in Krebs-Hanseleit buffer pH7.4 containing 0.5 mM L-carnitine and 5 mM HEPES. *: $p<0.05$

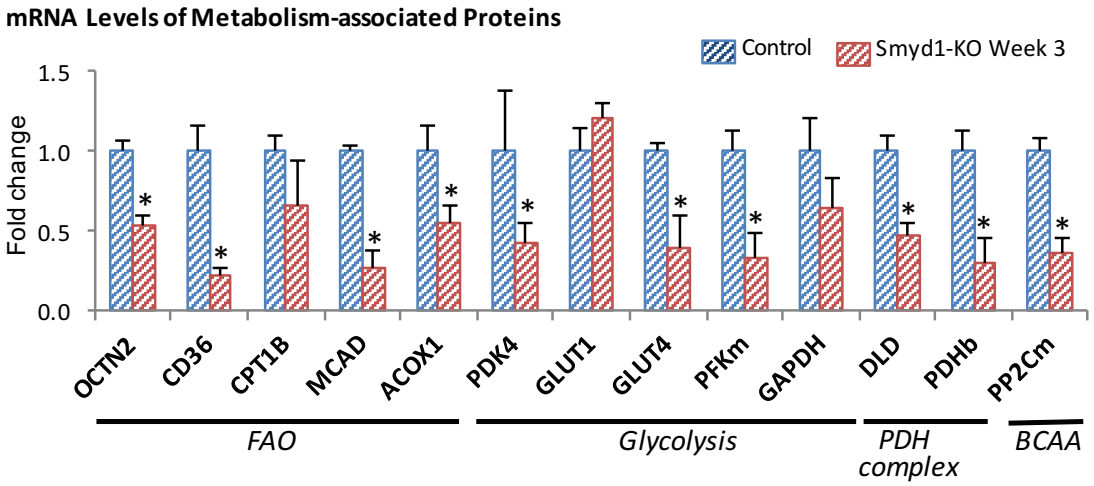

Fig. S4. Gene expression profile of Smyd1-KO mice at week 3. mRNA levels in control and Smyd1-KO hearts were normalized to Tbp transcript levels (n=4 in each group). Values represent fold changes relative to control, which was assigned as 1. FAO: fatty acid oxidation; PDH: pyruvate dehydrogenase; BCAA: branched-chain amino acid, *: $p<0.05$

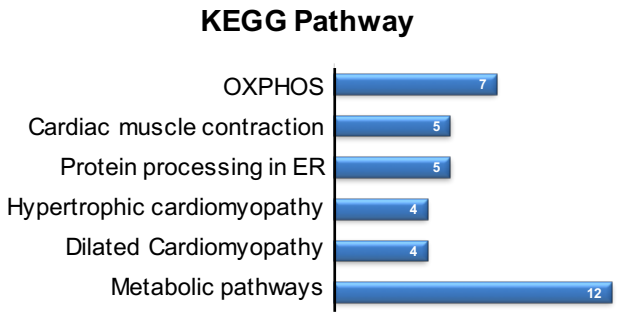

Fig. S5. KEGG pathways that were most affected by siRNA-mediated gene silencing of Smyd1 in NRVMs. Label-free proteomic analysis was performed using NRVMs that were transfected with either scrambled-siRNA (control) or Smyd1-siRNA (Smyd1-KD) for 48 hours. Among 1,421 proteins detected, 77 proteins were significantly changed by siRNA-mediated Smyd1-KD ($p<0.01$) which were analyzed for KEGG pathways using the STRING Database web-based tools. The KEGG pathways related to mitochondrial diseases (Parkinson's disease, Huntington's disease; Alzheimer's disease) and non-alcoholic fatty liver diseases were omitted as obviously irrelevant. The data can be found in the Supplemental Dataset S7.

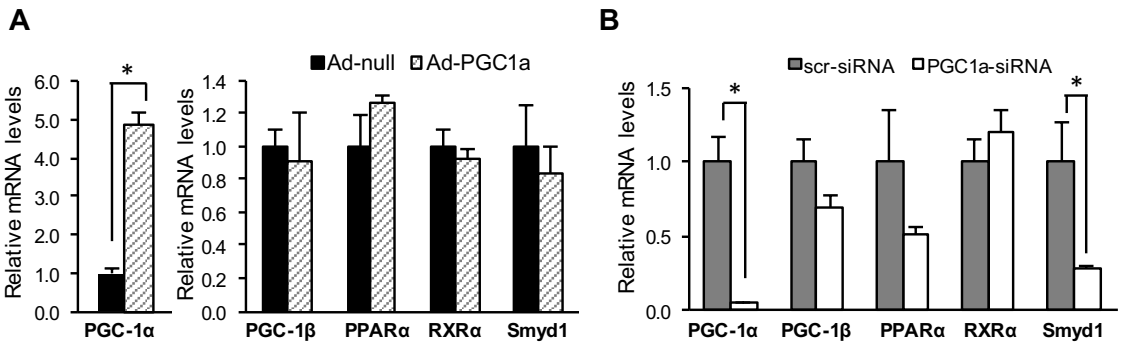

Fig. S6. Gene expression levels of PGC-1α, PGC-1β, PPARα, RXRα, and Smyd1 in H9c2 cardiomyocytes that were transduced with Ad-PGC1α (A) and that were transfected with PGC-1α-siRNA (B). mRNA levels in control (either Ad-null or scr-siRNA) and PGC-1α overexpressed/knockdown cells were normalized to Tbp transcript levels (n=3 in each group). Values represent fold changes relative to control, which was assigned as 1. *: $p<0.05$

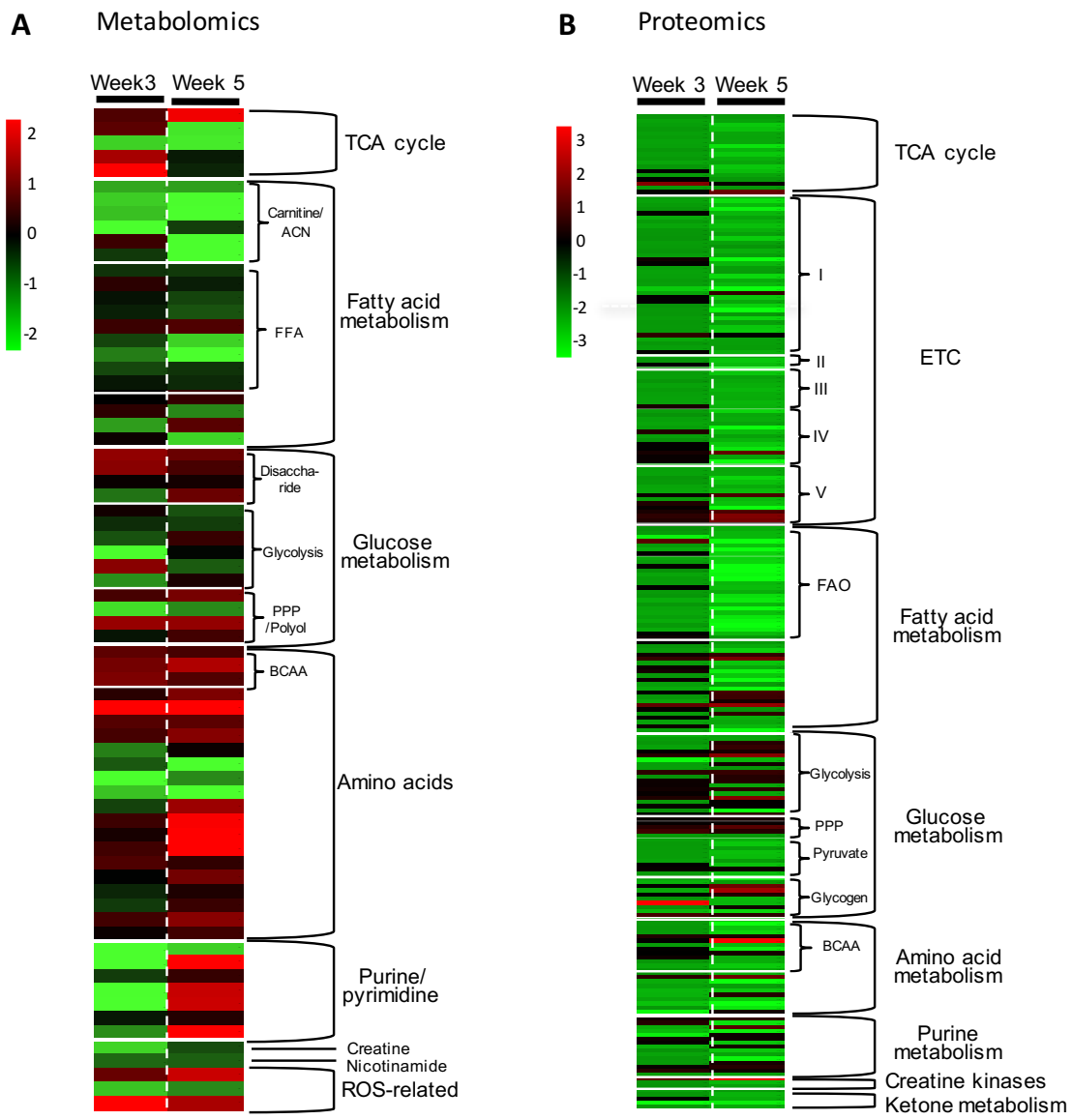

Fig. S7. Comparative analysis of metabolomic and proteomic profiles representing energy metabolic pathways in Smyd1-KO hearts at week 3 and week 5. A, All metabolites that belong to energy metabolic pathways are displayed in heat map format (*red* is increased, *green* decreased and *black* unchanged). **B,** Proteins that are associated with energy metabolism are displayed in the heat map. (*red* is upregulated, *green* downregulated and *black* unchanged). The intensity of color indicates the magnitude of the fold change with respect to control mice.

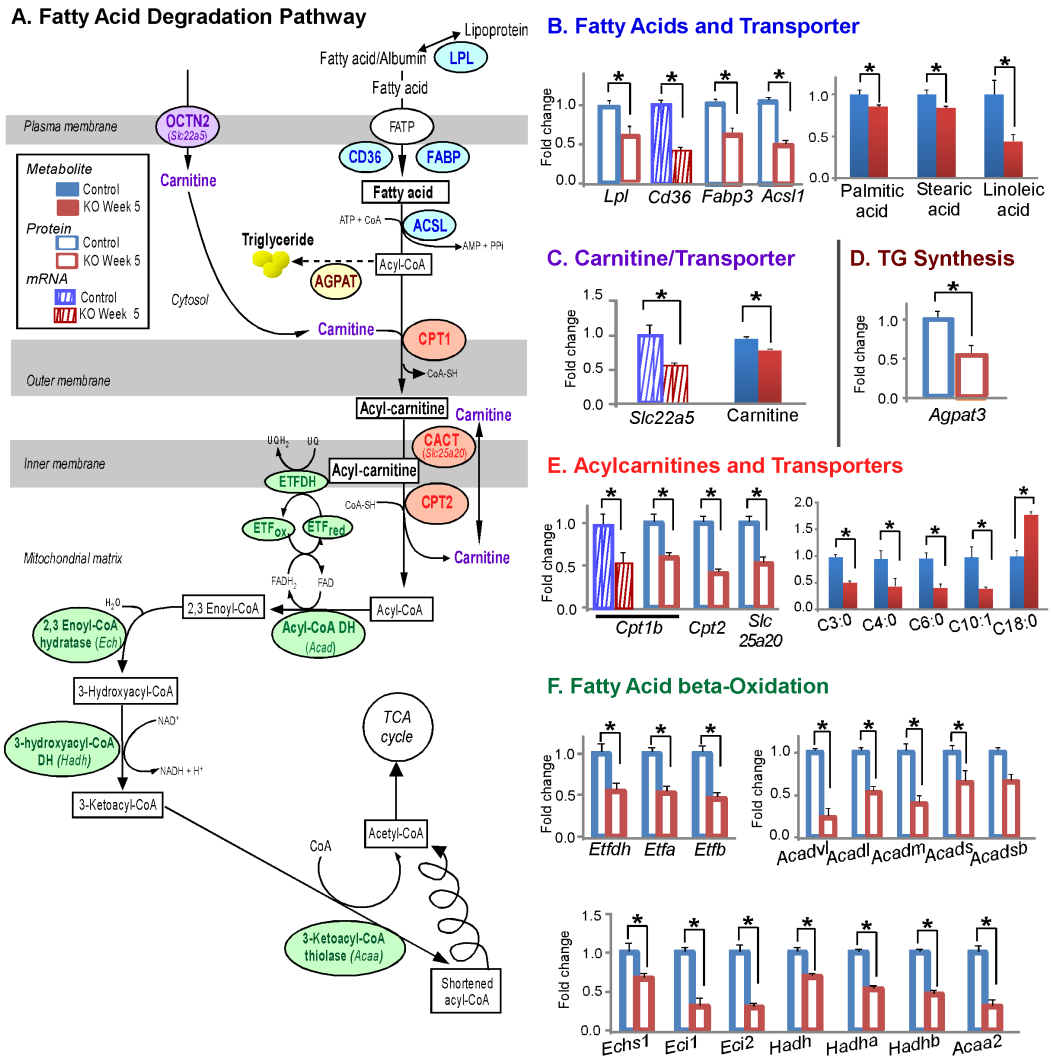

Fig. S8. Integrated view of alterations in fatty acid transport and oxidation caused by Smyd1-KO deletion at week 5 of tamoxifen treatment. A, Schematic diagram of fatty acid degradation pathway, showing all the detected proteins in the primary steps (cellular uptake and acetyl-CoA synthesis, *blue*), carnitine uptake (*purple*), carnitine shuttle (*orange*), and fatty acid β-oxidation (*green*). **B-F,** Combined information about proteins (open bars), metabolites (solid bars) and mRNA levels of selected genes (striped bars) that were significantly changed in the Smyd1-KO (*: $p<0.01$ for proteins, *: $p<0.05$ for metabolites and mRNA). Significantly altered proteins/metabolites were all downregulated/decreased, except the increased level of a long-chain acylcarnitine C18:0. OCTN2: organic cation transporter novel type 2, FATP: fatty acid transport protein, FABP: fatty acid binding protein, CPT1: carnitine palmitoyltransferase I, CPT2: carnitine palmitoyltransferase II, CACT: carnitine O-acetyltransferase; DH: dehydrogenase; ETF: electron-transferring flavoprotein; ETFDH: electron transfer flavoprotein-ubiquinone oxidoreductase.

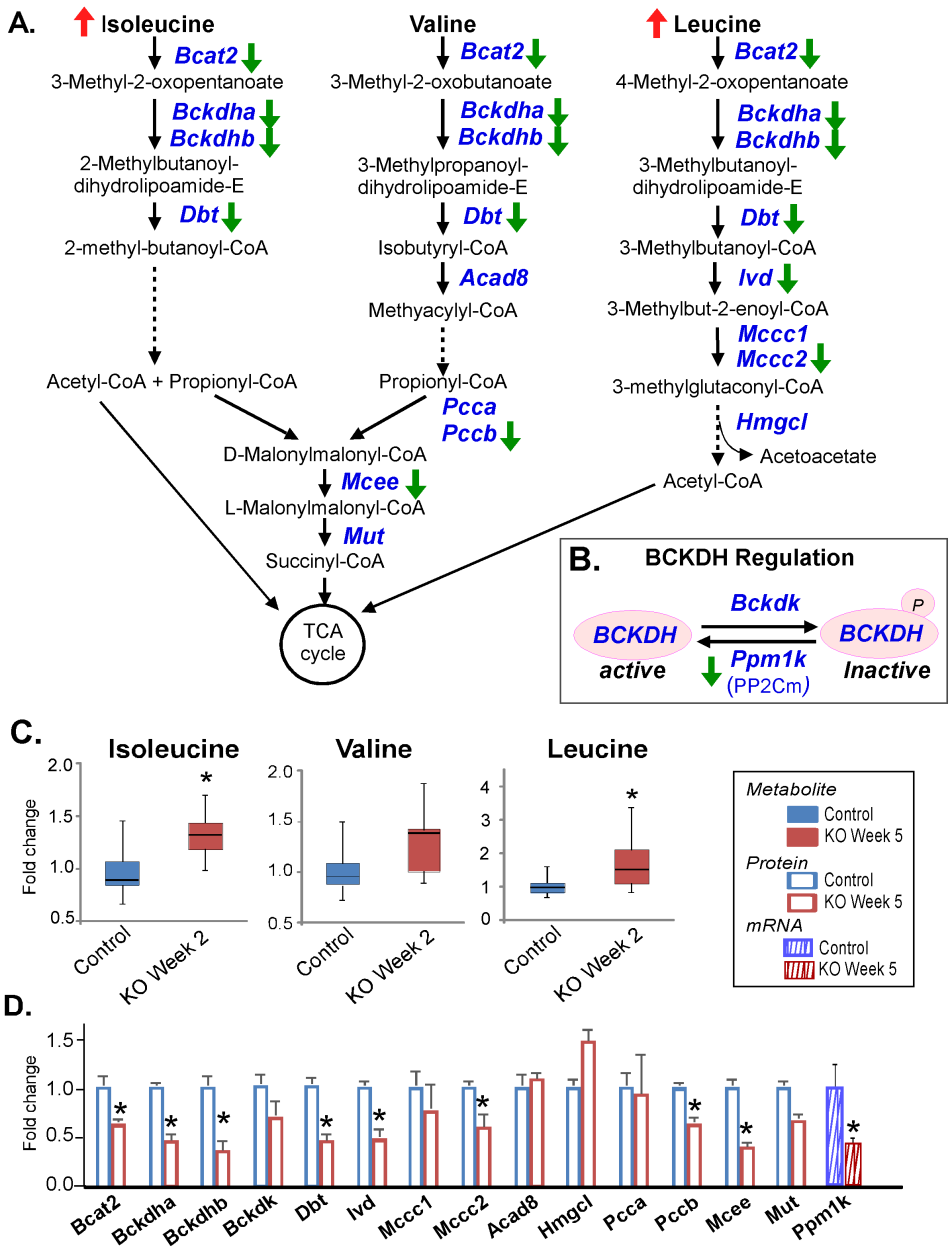

Fig. S9. Integrated view of alterations in BCAA degradation pathway caused by Smyd1-KO deletion at week 5 of tamoxifen treatment. A, Diagram of BCAA degradation pathway with arrows indicating the increased (*red*) or decreased (*green*) levels of metabolites and proteins in Smyd1-KO. **B,** Diagram depicting regulation of branched-chain α-keto acid dehydrogenase (BCKDH) by phosphorylation/dephosphorylation. BCKDH kinase (*Bckdk*) deactivates BCKDH activity through phosphorylation, while the mitochondrial phosphatase PP2Cm *(Ppm1k*) activates BCKDH through dephosphorylation. RT-PCR analysis reveals downregulation of *Ppm1k* in Smyd1-KO. **C,** Box-and-whisker plots of isoleucine, valine, and leucine show the accumulation of myocardial BCAAs in the KO (*: $p<0.05$, $p=0.056$ for valine). **D,** Protein (open bars) and mRNA levels (striped bars) of enzymes involved in BCAA degradation were mostly decreased in the KO (9 out of 15 analyzed enzymes, *$p<0.01$ and FC>1.5).

Dataset S1. Metabolomic data of Smyd1-KO mice at week 3.

Dataset S2. Proteomic data of Smyd1-KO mice at week 3 (all proteins)

Dataset S3. Proteomic data of Smyd1-KO mice at week 3 ($p<0.01$)

Dataset S4. GO analysis for cellular component enrichment analysis of the proteins that were differentially expressed in Smyd1-KO mice (week 3) compared with control mice.

Dataset S5. KEGG pathway enrichment analysis of the proteins that were differentially expressed in Smyd1-KO mice (week 3) compared with control mice.

Dataset S6. Proteomic data of NRVMs that were transfected with scrambled-siRNA (control) and Smyd1-siRNA (Smyd1-KD)

Dataset S7. KEGG pathway enrichment analysis of the proteins that were differentially expressed in Smyd1-KD NRVMs compared with control (scrambled-siRNA).

Dataset S8. Metabolomic data from Smyd1-KO mice at week 5

Dataset S9. Proteomic data from Smyd1-KO mice at week 5

Dataset S10. Proteomic data from Smyd1-KO mice at week 5 ($p<0.01$)

Dataset S11. KEGG pathway enrichment analysis of the proteins that were differentially expressed in Smyd1-KO mice (week 5) compared with control mice.

References

1. Franklin S, et al. (2016) The chromatin binding protein Smyd1 restricts adult mammalian heart growth. American journal of physiology. Heart and circulatory physiology:ajpheart 00235 02016.
2. Shibayama J, et al. (2015) Metabolic remodeling in moderate synchronous versus dyssynchronous pacing-induced heart failure: integrated metabolomics and proteomics study. PloS one 10(3):e0118974.
3. Pasikanti KK, Ho PC, & Chan ECY (2008) Gas chromatography/mass spectrometry in metabolic profiling of biological fluids. Journal of Chromatography B 871(2):202-211.
4. Meissen JK, et al. (2012) Induced pluripotent stem cells show metabolomic differences to embryonic stem cells in polyunsaturated phosphatidylcholines and primary metabolism. PloS one 7(10):e46770.
5. Cajka TF, O. (2016) Increasing lipidomic coverage by selecting optimal mobile-phase modifiers in LC–MS of blood plasma. Metabolomics 12(34).
6. Ghobakhlou A, et al. (2013) Metabolomic analysis of cold acclimation of Arctic Mesorhizobium sp. strain N33. PloS one 8(12):e84801.
7. Xia J, Psychogios N, Young N, & Wishart DS (2009) MetaboAnalyst: a web server for metabolomic data analysis and interpretation. Nucleic Acids Res 37(Web Server issue):W652-660.
8. Xia J, Mandal R, Sinelnikov IV, Broadhurst D, & Wishart DS (2012) MetaboAnalyst 2.0--a comprehensive server for metabolomic data analysis. Nucleic Acids Res 40(Web Server issue):W127-133.
9. Franceschini A, et al. (2013) STRING v9.1: protein-protein interaction networks, with increased coverage and integration. Nucleic acids research 41(Database issue):D808-815.
10. Rivals I, Personnaz L, Taing L, & Potier MC (2007) Enrichment or depletion of a GO category within a class of genes: which test? Bioinformatics 23(4):401-407.
11. Benjamini Y, Drai D, Elmer G, Kafkafi N, & Golani I (2001) Controlling the false discovery rate in behavior genetics research. Behavioural brain research 125(1-2):279-284.
12. Boudina S, et al. (2009) Contribution of impaired myocardial insulin signaling to mitochondrial dysfunction and oxidative stress in the heart. Circulation 119(9):1272-1283.
13. Cheung KG, et al. (2015) Sirtuin-3 (SIRT3) Protein Attenuates Doxorubicin-induced Oxidative Stress and Improves Mitochondrial Respiration in H9c2 Cardiomyocytes. The Journal of biological chemistry 290(17):10981-10993.
14. Kam Y JN, Clayton J, Held P, Dranka BP (2017) Normalization of Agilent Seahorse XF Data by In-situ Cell Counting Using a BioTek Cytation 5. Application Note by Agilent Technologies.
15. Shibayama J, et al. (2013) Metabolic determinants of electrical failure in ex-vivo canine model of cardiac arrest: evidence for the protective role of inorganic pyrophosphate. PloS one 8(3):e57821.
16. Bugger H, et al. (2010) Proteomic remodelling of mitochondrial oxidative pathways in pressure overload-induced heart failure. Cardiovascular research 85(2):376-384.